Scaling functions of interfacial tensions for a class of Ising cylinders

T. M. Liaw
Department of Physics, Chung-Yuan Christian University, Chungli 320, Taiwan
and Computing Centre and Institute of Physics, Academia Sinica, Nankang 115, Taiwan

M. C. Huang
Department of Physics, Chung-Yuan Christian University, Chungli 320, Taiwan

S. C. Lin
Department of Physics, Chung-Yuan Christian University, Chungli 320, Taiwan
and Computing Centre and Institute of Physics, Academia Sinica, Nankang 115, Taiwan

M. C. Wu
Department of Physics, Chung-Yuan Christian University, Chungli 320, Taiwan
(Received 3 March 1999)

We apply Plechko's Grassmann path-integral method to Ising cylinders of rectangular, triangular, and hexagonal lattices to obtain the analytic solutions of free energies for the periodic and antiperiodic boundary conditions in the joined circumferences of the cylinders. These analytic solutions are used to analyze the scaling functions of the interfacial tensions for isotropic and anisotropic couplings. The finite-size corrections to the scaling functions are also discussed. [S0163-1829(99)12141-6]

I. INTRODUCTION

There is extensive current interest in the properties of surfaces and interfaces near the bulk critical point in both theory and experiment. The interfacial free energy is defined as the difference of two finite-size systems with different boundary conditions. For the case of the Ising model, the difference in free energy between a system with periodic and antiperiodic boundary conditions is sometimes referred to as the Bloch wall free energy, and few results[1,2,3] exist for the properties of the free energy of an infinitely extended Block wall. In this paper we analyze the properties, mainly the scaling functions, of the Bloch wall free energies of infinitely long Ising cylinders of square, triangular, and hexagonal lattices, based on the analytic solutions of the free energies.

The analytic solution of the Ising model on a square lattice was first solved by Onsager in the limit of an infinitely large lattice using the theory of Lie algebra.[4] This method was simplified by Kaufman[5] using the theory of spinor representation. Then Schultz, Mattis, and Lieb[6] gave explicitly the fermionic treatment. The other alternative is the combinatorial method, which was first developed by Kac and Ward[7] and then rigorously reformulated by Hurst and Green.[8] More recently Plechko used a nonstandard and relatively simple approach to obtain analytic expressions of the partition functions for the Ising model on a torus,[9] a class of triangular-type decorated lattices,[10] and a triangular lattice net with holes.[11] This method is based on the Grassmann path-integral factorization of the Boltzmann weights along with the principle of mirror ordering of the arising Grassmann factors. Here traditional transfer matrix or combinatorial considerations used in the previous methods are not needed. In this paper, we work in this framework to obtain analytic solutions of the partition functions for infinitely long cylinders of square, triangular, and hexagonal lattices with periodically or antiperiodically joined circumferences. Then we use these solutions to find the interfacial tensions, and to study the scaling functions of the interfacial tensions for different coupling ratios.

This paper is organized as follows. In Sec. II, we set up a general form of the partition function of the Ising model that can be applied to square, triangular, and hexagonal lattices. In Sec. III, we first introduce three pairs of conjugate Grassmann variables for a lattice site to factorize the Boltzmann weights, and then we use the principle of mirror ordering to rearrange the Grassmann factors so we can perform the summation over Ising spins to obtain a pure fermionic expression of the partition function. In Sec. IV, using the Fourier transform technique we complete the integrations over the Grassmann variables to obtain the analytic solutions of the free energies. In Sec. V, we use the free energies obtained in the last section to study the scaling functions of the interfacial tensions for different coupling ratios. Finally, Sec. VI is reserved for the summary of the results.

II. GENERALIZED PARTITION FUNCTION

In this section, starting with a triangular lattice we set up a generalized partition function of the Ising model that can be applied to rectangular, triangular, and hexagonal lattices.

Consider a triangular lattice with site identifications shown in Fig. 1. The partition function is written as

$$Z=\sum_{\{\sigma\}} e^{-\beta H}, \tag{1}$$

where β is the inverse of the reduced temperature $\beta=1/(k_BT)$, H is the Hamiltonian defined as

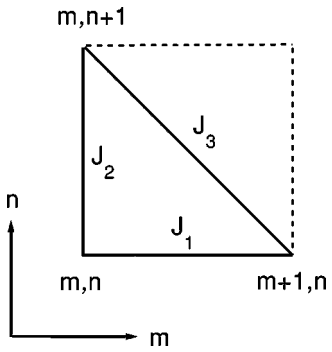

FIG. 1. A basic cell in the type of triangular lattices used in this work. A lattice site is given by (m,n), and the coupling constants are J_1, J_2, and J_3.

$$H=-\sum_{m,n}\left(J_1\sigma_{m,n}\sigma_{m+1,n}+J_2\sigma_{m,n}\sigma_{m,n+1}+J_3\sigma_{m+1,n}\sigma_{m,n+1}\right), \tag{2}$$

J_i with $i=1,2,3$ is the coupling constant, and $\sigma_{m,n}$ is the Ising spin defined on the site (m,n) and it has two possible values, $+1$ and -1. Using the identity,

$$e^{\beta J_i\sigma_j\sigma_k}=(1-t_i^2)^{-1/2}(1+t_i\sigma_j\sigma_k), \tag{3}$$

with $t_i=\tanh(\beta J_i)$, we can rewrite the partition function as

$$Z_T=R_T^{N_T}\prod_{m,n}\frac{1}{2}\sum_{\sigma_{m,n}}(1+r_1^T\sigma_{m,n}\sigma_{m+1,n})(1+r_2^T\sigma_{m,n}\sigma_{m,n+1})\times(1+r_3^T\sigma_{m+1,n}\sigma^{m,n+1}), \tag{4}$$

where N_T is the total number of lattice sites of a triangular lattice,

$$R_T=2\prod_{i=1}^{3}(1-t_i^2)^{-1/2}, \tag{5}$$

and $r_i^T=t_i$ with $i=1,2,3$. Note that this partition function can be transformed to the one on a rectangular lattice by setting $t_3=0$.

For the case of a hexagonal lattice, we note that one can use the star-triangle transformation to transform a hexagonal to a triangular lattice as shown in Fig. 2. First we can express the Hamiltonian as

$$H=-\sum_{m,n}\left(J_1\sigma_0\sigma_{m,n}+J_2\sigma_0\sigma_{m,n+1}+J_3\sigma_0\sigma_{m+1,n}\right), \tag{6}$$

where σ_0 denotes the Ising spins indicated in Fig. 2. Then using the identity of Eq. (3), we can obtain the partition function as

$$Z_H=R_H^{N_H}\prod_{m,n}\frac{1}{2}\sum_{\sigma_{m,n}}\left\{\frac{1}{2}\sum_{\sigma_0}(1+t_1\sigma_0\sigma_{m,n})(1+t_2\sigma_0\sigma_{m,n+1})\times(1+t_3\sigma_0\sigma_{m+1,n})\right\}, \tag{7}$$

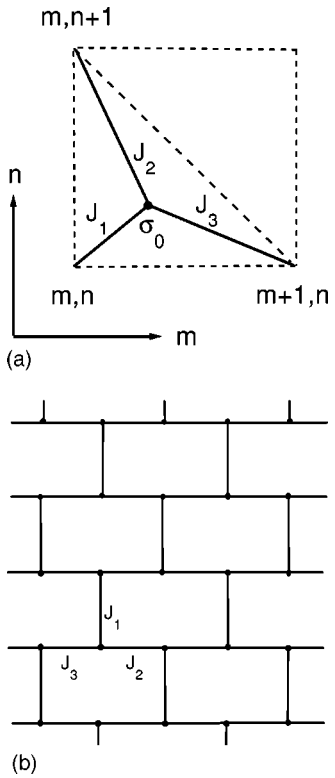

FIG. 2. (a) The basic cell in the type of hexagonal lattices used in this work. There is no position specification at the location of the Ising spin σ_0. (b) The equivalent structure of the hexagonal lattice.

where $N_H(=2N_T)$ is the total number of lattice sites of a hexagonal lattice, and $R_H=2R_T$. After performing the sum over σ_0, the partition function becomes

$$Z_H=R_H^{N_H}\prod_{m,n}\frac{1}{2}\sum_{\sigma_{m,n}}\left(\alpha_0+\alpha_1\sigma_{m,n}\sigma_{m+1,n}+\alpha_2\sigma_{m,n}\sigma_{m,n+1}+\alpha_3\sigma_{m+1,n}\sigma_{m,n+1}\right), \tag{8}$$

with

$$\alpha_0=1,\ \alpha_1=t_1t_3,\ \alpha_2=t_1t_2,\ \text{and}\ \alpha_3=t_2t_3. \tag{9}$$

The above partition function can be reparametrized in a form similar to Eq. (4), and the resultant form is

$$Z_H=R_H^{N_H}\prod_{m,n}\frac{1}{2}\sum_{\sigma_{m,n}}\{r_0^H(1+r_1^H\sigma_{m,n}\sigma_{m+1,n})\times(1+r_2^H\sigma_{m,n}\sigma_{m,n+1})\times(1+r_3^H\sigma_{m+1,n}\sigma_{m,n+1})\}, \tag{10}$$

where r_i^H with $i=0,1,2,3$ is determined by the relations

$$\alpha_0=r_0^H(1+r_1^Hr_2^Hr_3^H),\quad \alpha_1=r_0^H(r_1^H+r_2^Hr_3^H),$$
$$\alpha_2=r_0^H(r_2^H+r_1^Hr_3^H),\quad \alpha_3=r_0^H(r_3^H+r_1^Hr_2^h). \tag{11}$$

From Eqs. (4) and (10), we can define the generalized reduced partition function as

$$Q=\prod_{m=1}^{L_x}\prod_{n=1}^{L_y}\frac{1}{2}\sum_{\sigma_{m,n}}P_{m,n}(\sigma), \tag{12}$$

where $P_{m,n}(\sigma)$ take the form

$$P_{m,n}(\sigma)=(1+r_1\sigma_{m,n}\sigma_{m+1,n})(1+r_2\sigma_{m,n}\sigma_{m,n+1}) \times(1+r_3\sigma_{m,n+1}\sigma_{m+1,n}), \tag{13}$$

and the parameters r_i with $i=1,2,3$ vary from one lattice to the other.

III. FERMIONIC EXPRESSION OF PARTITION FUNCTION

In this section, first we introduce a set of anticommuting Grassmann variables for each lattice site to express the generalized reduced partition function Q of Eq. (12) as a mixed representation of spin and Grassmann variables. In this mixed representation, a Boltzmann weight in Eq. (12) is decoupled to the product of two factors of separated spins. Then by using the technique of the mirror-ordered factorization, we can group the factors containing the same spin together to perform the sum over spins. After eliminating the spin variables we obtain a purely fermionic expression of Q that is a multidimensional Gaussian integral. The boundary condition we use is defined as follows: For the y direction we first set $\sigma_{m,1}=\sigma_{m,L_y+1}=0$ and then take the limit of $L_y\rightarrow\infty$, and for the x direction we set $\sigma_{L_x+1,n}=k\sigma_{1,n}$ with $k=1$ for the periodic boundary condition and $k=-1$ for the antiperiodic boundary condition. Thus the solution we obtain corresponds to the case of an Ising cylinder infinitely extending in the y direction and rounding periodically or antiperiodically in the x direction.

Three pairs of conjugate Grassmann variables, $\{a_{m,n},a^*_{m,n};b_{m,n},b^*_{m,n};c_{m,n},c^*_{m,n}\}$, are defined on a lattice site (m,n). All Grassmann variables anticommute, and their squares are zeros. The basic rules of integration for one Grassmann variable are defined as

$$\int da_{m,n}\cdot 1=0 \quad\text{and}\quad \int da_{m,n}\cdot a_{m,n}=1. \tag{14}$$

This definition can be viewed as the consequence of proper normalization and transnational invariance, namely

$$\int da_{m,n}\cdot\Omega(a_{m,n}+\eta)=\int da_{m,n}\cdot\Omega(a_{m,n}), \tag{15}$$

for an arbitrary anticommuting complex number η.[12] Also the symbols of the differentials anticommute with each other and with the variables. For each pair of conjugate variables introduced above, say $a_{m,n}$ and $a^*_{m,n}$, we follow Plechko's notation to define the average of an arbitrary function $f(a_{m,n},a^*_{m,n})$ with a Gaussian weight as

$$\operatorname*{Sp}_{(a_{m,n})}\{f(a_{m,n},a^*_{m,n})\} =\int da^*_{m,n}\int da_{m,n}e^{a_{m,n}a^*_{m,n}}f(a_{m,n},a^*_{m,n}). \tag{16}$$

Similar definitions are used for $b_{m,n}$ and $b^*_{m,n}$, and $c_{m,n}$ and $c^*_{m,n}$. We also define the total average over all these pairs as

$$\operatorname*{Sp}_{(a,b,c)}\{g(a,a^*;b,b^*;c,c^*)\}=\prod_{m=1}^{L_x}\prod_{n=1}^{L_y}\operatorname*{Sp}_{(a_{m,n})}\operatorname*{Sp}_{(b_{m,n})}\operatorname*{Sp}_{(c_{m,n})} \times\{g(a,a^*;b,b^*;c,c^*)\}. \tag{17}$$

Using these Grassmann variables, we can rewrite $P_{m,n}(\sigma)$ of Eq. (13) as

$$P_{m,n}(\sigma)=\operatorname*{Sp}_{(a_{m,n})}\operatorname*{Sp}_{(b_{m,n})}\operatorname*{Sp}_{(c_{m,n})} \times\{A_{m,n}A^*_{m+1,n}B_{m,n}B^*_{m,n+1}C_{m,n+1}C^*_{m+1,n}\}, \tag{18}$$

where the Grassmann factors, A,A^*,B,B^*,C, and C^* are defined as

$$A_{m,n}=1+a_{m,n}\sigma_{m,n},\quad A^*_{m,n}=1+r_1a^*_{m-1,n}\sigma_{m,n}, \tag{19}$$

$$B_{m,n}=1+b_{m,n}\sigma_{m,n},\quad B^*_{m,n}=1+r_2b^*_{m,n-1}\sigma_{m,n}, \tag{20}$$

and

$$C_{m,n}=1+c_{m,n-1}\sigma_{m,n},\quad C^*_{m,n}=1+r^*_{m-1,n}\sigma_{m,n}. \tag{21}$$

Here a Boltzmann weight in Eq. (12) is decoupled to the product of two factors of separated spins. Then by substituting Eq. (18) into Eq. (12) and by using the fact that $C_{m,n+1}C^*_{m+1,n}$ for given m and n is commutable with Grassmann variables inside the Grassmann integral, we can express the partition function as

$$Q=\operatorname*{Sp}_{(a,b,c)}\left\{\prod_{m=1}^{L_x}\prod_{n=1}^{L_y}\frac{1}{2}\sum_{\sigma_{m,n}}A_{m,n}C_{m,n+1} \times C^*_{m+1,n}A^*_{m+1,n}B_{m,n}B^*_{m,n+1}\right\}. \tag{22}$$

To group the factors containing the same spin variable together, we proceed by applying the principle of mirror ordering. To simplify the notation, we define

$$\Phi_{m,n}=A_{m,n}C_{m,n+1}\quad\text{and}\quad\Phi^*_{m+1,n}=C^*_{m+1,n}A^*_{m+1,n}. \tag{23}$$

By using the fact that the combination $\Phi_{m,n}\Phi^*_{m+1,n}$ taken as a whole is a commutable object inside the Grassmann integral, we can rewrite the partition function as

$$Q=\operatorname*{Sp}_{(a,b,c)}\left\{2^{-N_T}\sum_{\{\sigma\}}\left(\prod_{m=1}^{L_x}\prod_{n=1}^{L_y}\Phi_{m,n}\Phi^*_{m+1,n}\right) \times\left(\prod_{m=1}^{L_x}\prod_{n=1}^{L_y}B_{m,n}B^*_{m,n+1}\right)\right\}. \tag{24}$$

To factorize out the boundary terms, we can reexpress Eq. (24) as

$$Q=\operatorname*{Sp}_{(a,b,c)}\left\{2^{-N_T}\sum_{\{\sigma\}}\left(\prod_{m=1}^{L_x-1}\prod_{n=1}^{L_y}\Phi_{m,n}\Phi^*_{m+1,n}\right)\times\Psi_B\cdot\left(\prod_{m=1}^{L_x}\prod_{n=1}^{L_y-1}B_{m,n}B^*_{m,n+1}\right)\right\},\tag{25}$$

with Ψ_B, the boundary terms,

$$\Psi_B=\left(\prod_{n=1}^{L_y}\overrightarrow{\Phi_{L_x,n}}^{\,n}\right)\left(\prod_{n=1}^{L_y}\overleftarrow{\Phi^*_{L_x+1,n}}^{\,n}\right)\left(\prod_{m=1}^{L_x}\overleftarrow{B_{m,L_y}}^{\,m}\right).\tag{26}$$

Here the two products in n are ordered in opposite direction as indicated by the arrows, and similarly the order of the product in m is also indicated by an arrow. Note that in obtaining Eq. (26), first we use the fact that the combination $\Phi_{L_x,n}\Phi^*_{L_x+1,n}$ taken as a whole is a commutable object. We have the order in n shown by the arrows, and then also using the property of commutability we arrange the product of $B_{m,L_y}B^*_{m,L_y+1}$ in m to have the order shown by an arrow, and finally we use the boundary condition $\sigma_{m,L_y+1}=0$ to set $B^*_{m,L_y+1}=1$. Subject to the boundary condition $\sigma_{L_x+1,n}=k\sigma_{1,n}$ with $k=1$ or -1, we have to impose the identifications

$$a^*_{0,n}=-ka^*_{L,n}\ \text{ and }\ c^*_{0,n}=-kc^*_{L,n},\tag{27}$$

as the boundary conditions of the Grassmann variables so that we can rewrite the boundary terms as

$$\Psi_B=\left(\prod_{n=1}^{L_y}\overleftarrow{\Phi^*_{1,n}}^{\,n}\right)\left(\prod_{n=1}^{L_y}\overrightarrow{\Phi_{L_x,n}}^{\,n}\right)\left(\prod_{m=1}^{L_x}\overleftarrow{B_{m,L_y}}^{\,m}\right).\tag{28}$$

which have the mirror-ordered form for the terms in the first two brackets. To further simplify the notation, we define

$$\overrightarrow{\Theta}^{\,n}_m=\prod_{n=1}^{L_y}\overrightarrow{\Phi_{m,n}}^{\,n}\ \text{ and }\ \overleftarrow{\Theta^*_m}^{\,n}=\prod_{n=2}^{L_y}\overleftarrow{\Phi^*_{m,n}}^{\,n}.\tag{29}$$

Then substituting Ψ_B of Eq. (28) into Eq. (25) and using the fact that $\overrightarrow{\Theta}^{\,n}_m\ \overleftarrow{\Theta^*_{m+1}}^{\,n}$ as a whole is a commutable object to insert it between $\overleftarrow{\Theta^*_1}^{\,n}$ and $\overrightarrow{\Theta}^{\,n}_{L_s}$ for $m=1$ to L_x-1 properly, we can rewrite the partition function as

$$Q=\operatorname*{Sp}_{(a,b,c)}\left\{2^{-N_T}\sum_{\{\sigma\}}\left(\prod_{m=1}^{L_x}\overleftarrow{\Theta^*_m}^{\,n}\overrightarrow{\Theta}^{\,n}_m\right)\left(\prod_{m=1}^{L_x}\overleftarrow{B_{m,L_y}}^{\,m}\right)\times\left(\prod_{m=1}^{L_x}\prod_{n=1}^{L_y-1}B_{m,n}B^*_{m,n+1}\right)\right\},\tag{30}$$

To have a complete mirror-ordered form, we have to rearrange the terms in the last two brackets. To achieve this, first we use Eqs. (23) and (29) to express $\overrightarrow{\Theta}^{\,n}_m$ as

$$\overrightarrow{\Theta}^{\,n}_m=\left(\prod_{n=1}^{L_y-1}\overrightarrow{A_{m,n}C_{m,n+1}}^{\,n}\right)A_{m,L_y}C_{m,L_y+1},\tag{31}$$

with $C_{m,L_y+1}=1$. Then by using the fact that $B_{m,n}B^*_{m,n+1}$ as a whole for given m and n is a commutable object inside the Grassmann integral, we can have the insertion of $B_{m,n}B^*_{m,n+1}$ between $A_{m,n}$ and $C_{m,n+1}$ of $\overrightarrow{\Theta}^{\,n}_m$ to obtain the expression

$$Q=\operatorname*{Sp}_{(a,b,c)}\left\{2^{-N_T}\sum_{\{\sigma\}}\prod_{m=1}^{L_x}\left[\overleftarrow{\Theta^*_m}^{\,n}\left(\prod_{n=1}^{L_y-1}\overrightarrow{A_{m,n}B_{m,n}B^*_{m,n+1}C_{m,n+1}}^{\,n}\right)A_{m,L_y}\right]\left(\prod_{m=1}^{L_x}\overleftarrow{B_{m,L_y}}^{\,m}\right)\right\}.\tag{32}$$

By using the boundary condition $\sigma_{m,1}=0$ to set $A_{m,1}=B_{m,1}=1$, we can rearrange the above equation to yield

$$Q=\operatorname*{Sp}_{(a,b,c)}\left\{2^{-N_T}\sum_{\{\sigma\}}\prod_{m=1}^{L_x}\left[\overleftarrow{\Theta^*_m}^{\,n}\left(\prod_{n=2}^{L_y-1}\overrightarrow{B^*_{m,n}C_{m,n}A_{m,n}B_{m,n}}^{\,n}\right)B^*_{m,L_y}C_{m,L_y}A_{m,L_y}\right]\left(\prod_{m=1}^{L_x}\overleftarrow{B_{m,L_y}}^{\,m}\right)\right\}.\tag{33}$$

Now it is straightforward to show that the partition function given in the above is equivalent to

$$Q=\operatorname*{Sp}_{(a,b,c)}\left\{\prod_{m=1}^{L_x}\prod_{n=2}^{L_y}\frac{1}{2}\sum_{\sigma_{m,n}}C^*_{m,n}A^*_{m,n}B^*_{m,n}C_{m,n}A_{m,n}B_{m,n}\right\}.\tag{34}$$

First we consider the term of $m=L_x$ in Eq. (33) denoted by T,

$$T=\sum_{\{\sigma\}}\left[\overleftarrow{\Theta^*_{L_x}}^{\,n}\left(\prod_{n=2}^{L_y-1}\overrightarrow{B^*_{L_x,n}C_{L_x,n}A_{L_x,n}B_{L_x,n}}^{\,n}\right)\times B^*_{L_x,L_y}C_{L_x,L_y}A_{L_x,L_y}B_{L_x,L_y}\right],\tag{35}$$

By substituting Eq. (29) into Eq. (35), we have

$$T=\sum_{\{\sigma\}}\left[\left(\prod_{n=2}^{L_y}\overleftarrow{C^*_{L_x,n}A^*_{L_x,n}}^{\,n}\right)\times\left(\prod_{n=2}^{L_y}\overrightarrow{B^*_{L_x,n}C_{L_x,n}A_{L_x,n}B_{L_x,n}}^{\,n}\right)\right], \quad (36)$$

which is equivalent to the form

$$T=\prod_{n=2}^{L_y}\sum_{\sigma_{L_x,n}}(C^*_{L_x,n}A^*_{L_x,n}B^*_{L_x,n}C_{L_x,n}A_{L_x,n}B_{L_x,n}), \quad (37)$$

inside the Grassmann integration due to the fact that after summing over spin, the factor $\Sigma_{\sigma_{L_x,n}}(C^*_{L_x,n}A^*_{L_x,n}B^*_{L_x,n}C_{L_x,n}A_{L_x,n}B_{L_x,n})$, for a given n is an even polynomial in Grassmann variables and becomes a commutable object. Note that in obtaining Eq. (37), we use the boundary condition $\sigma_{m,1}=0$ to set $C^*_{L_x,1}A^*_{L_x,1}=1$. Then by continuing such construction from $m=L_x$ down to $m=1$, we can obtain the expression of Eq. (34).

For the partition function given by Eq. (34), the factors containing the same spin are grouped together and we can perform the sum over spins. Note that for two Grassmann variables g_1 and g_2, we can use the identities $\sigma^2=1$ and $e^{g_1g_2}=1+g_1g_2$, to obtain the formula

$$(1+g_1\sigma)(1+g_2\sigma)=e^{g_1g_2}[1+(g_1+g_2)\sigma], \quad (38)$$

and after summing over spin we have

$$\sum_{\sigma=\pm1}(1+g_1\sigma)(1+g_2\sigma)=2e^{g_1g_2}. \quad (39)$$

By using this formula to perform the sum over spins, we obtain the result

$$\frac{1}{2}\sum_{\sigma_{m,n}}C^*_{m,n}A^*_{m,n}B^*_{m,n}C_{m,n}A_{m,n}B_{m,n}=\exp(\tilde{G}_{m,n}), \quad (40)$$

with

$$\begin{aligned}\tilde{G}_{m,n}=&r_1r_3c^*_{m-1,n}a^*_{m-1,n}+(r_3c^*_{m-1,n}+r_1a^*_{m-1,n})r_2b^*_{m,n-1}\\&+(r_3c^*_{m-1,n}+r_1a^*_{m-1,n}+r_2b^*_{m,n-1})c_{m,n-1}\\&+(r_3c^*_{m-1,n}+r_1a^*_{m-1,n}+r_2b^*_{m,n-1}+c_{m,n-1})a_{m,n}\\&+(r_3c^*_{m-1,n}+r_1a^*_{m-1,n}+r_2b^*_{m,n-1}+c_{m,n-1}\\&+a_{m,n})b_{m,n}. \quad (41)\end{aligned}$$

Then we obtain a purely fermionic expression of Q,

$$Q=\int\prod_{m=1}^{L_x}\prod_{n=2}^{L_y}da^*_{m,n}da_{m,n}db^*_{m,n}db_{m,n}dc^*_{m,n}dc_{m,n}\times\exp\left(\sum_{m=1}^{L_x}\sum_{n=2}^{L_y}G_{m,n}\right), \quad (42)$$

where

$$G_{m,n}=a_{m,n}a^*_{m,n}+b_{m,n}b^*_{m,n}+c_{m,n}c^*_{m,n}+\tilde{G}_{m,n}. \quad (43)$$

Here the boundary condition is $a^*_{0,n}=-a^*_{L,n}$ and $c^*_{0,n}=-c^*_{L,n}$ for the periodic case, and $a^*_{0,n}=a^*_{L,n}$ and $c^*_{0,n}=c^*_{L,n}$ for the antiperiodic case.

IV. FREE ENERGY

In this section, starting with the fermionic expression of the generalized reduced partition function obtained in the last section, we use the technique of Fourier transform to complete the integration so that we can have the analytic solution of the reduced free energy.

The fermionic expression of the generalized reduced partition function Q given by Eq. (42) is a Gaussian integral of the Grassmann variables that mix together with the variables at different sites. To have a diagonal form, we make a Fourier transformation to obtain its momentum representation. The Fourier transformation is defined as

$$X_{m,n}=\frac{1}{\sqrt{L_xL^*_y}}\sum_{\bar{p},\bar{q}}X_{\bar{p},\bar{q}}e^{-t(2\pi/L_x)m\bar{p}}e^{-i(2\pi/L^*_y)n\bar{q}}, \quad (44)$$

and

$$X^*_{m,n}=\frac{1}{\sqrt{L_xL^*_y}}\sum_{\bar{p},\bar{q}}X^*_{\bar{p},\bar{q}}e^{i(2\pi/L_x)m\bar{p}}e^{t(2\pi/L^*_y)n\bar{q}}, \quad (45)$$

where the variable $X_{m,n}(X^*_{m,n})$ denotes one of the variables $\{a_{m,n},b_{m,n},c_{m,n}\}(\{a^*_{m,n},b^*_{m,n},c^*_{m,n}\})$, $L^*_y=L_y-1$, and $\bar{p}=p+\frac{1}{2}$ and $\bar{q}=q+\frac{1}{2}$ for the periodic case and $\bar{p}=p$ and $\bar{q}=q$ for the antiperiodic case with the integer p ranging from 1 to L_x and q from 2 to L_y-1. Note that owing to the free boundary condition for the y direction, which we used in obtaining Eq. (42) by setting $\sigma_{m,1}=\sigma_{m,L_y+1}=0$, the Fourier transforms defined by Eqs. (44) and (45) are exact only in the limit of $L_y\to\infty$. In this limit taking $\bar{q}$ to be either $q+\frac{1}{2}$ or q leads to the same result.

After performing the Fourier transformation, the partition function becomes

$$Q=\prod_{\bar{p},\bar{q}}Q_{\bar{p},\bar{q}}, \quad (46)$$

where $Q_{\bar{p},\bar{q}}$ is given by

$$Q_{\bar{p},\bar{q}}=\int dV_{\bar{p},\bar{q}}\exp(H_{\bar{p},\bar{q}}), \quad (47)$$

with the measure $dV_{\bar{p},\bar{q}}$ given by

$$dV_{\bar{p},\bar{q}}=da^*_{\bar{p},\bar{q}}da_{\bar{p},\bar{q}}db^*_{\bar{p},\bar{q}}db_{\bar{p},\bar{q}}dc^*_{\bar{p},\bar{q}}dc_{\bar{p},\bar{q}}, \quad (48)$$

and the function $H_{\bar{p},\bar{q}}$, given in Table I. Because $H_{\bar{p},\bar{q}}$ contains not only the variables $X_{\bar{p},\bar{q}}$ and $X^*_{\bar{p},\bar{q}}$, but also the variables $X_{L_x-\bar{p},L^*_y-\bar{q}}$ and $X^*_{L_x-\bar{p},L^*_y-\bar{q}}$, instead of calculating Q it is easier to calculate Q^2 given by

$$Q^2=\prod_{\bar{p},\bar{q}}Q^2_{\bar{p},\bar{q}}, \quad (49)$$

with

TABLE I. The terms contained in $H_{\overline{p},\overline{q}}$ of Eq (47) with $\hat{p}=2\pi\overline{p}/L_x$ and $\hat{q}=2\pi\overline{q}/L_y^*$. Each row with the coefficient in front of the variable represents a term appearing in $H_{\overline{p},\overline{q}}$.

Variable	Coefficient
$c^*_{\overline{p},\overline{q}}a^*_{L_x-\overline{p},L_y^*-\overline{q}}$	r_1r_3
$c_{\overline{p},\overline{q}}b^*_{L_x-\overline{p},L_y^*-\overline{q}}$	$r_2r_3e^{i(\hat{q}-\hat{p})}$
$a^*_{\overline{p},\overline{q}}b^*_{L_x-\overline{p},L_y^*-\overline{q}}$	$r_1r_2e^{i(\hat{q}-\hat{p})}$
$c_{\overline{p},\overline{q}}a_{L_x-\overline{p},L_y^*-\overline{q}}$	$e^{i\hat{q}}$
$c_{\overline{p},\overline{q}}b_{L_x-\overline{p},L_y^*-\overline{q}}$	$e^{i\hat{q}}$
$a_{\overline{p},\overline{q}}b_{L_x-\overline{p},L_y^*-\overline{q}}$	1
$c_{\overline{p},\overline{q}}c^*_{\overline{p},\overline{q}}$	$1-r_3e^{i(\hat{q}-\hat{p})}$
$a_{\overline{p},\overline{q}}a^*_{\overline{p},\overline{q}}$	$1-r_1e^{-i\hat{p}}$
$b_{\overline{p},\overline{q}}b^*_{\overline{p},\overline{q}}$	$1-r_2e^{-i\hat{q}}$
$c^*_{\overline{p},\overline{q}}a_{\overline{p},\overline{q}}$	$r_3e^{-i\hat{p}}$
$c^*_{\overline{p},\overline{q}}b_{\overline{p},\overline{q}}$	$r_3e^{-i\hat{p}}$
$a^*_{\overline{p},\overline{q}}c_{\overline{p},\overline{q}}$	$r_1e^{i(\hat{q}-\hat{p})}$
$a^*_{\overline{p},\overline{q}}b_{\overline{p},\overline{q}}$	$r_1e^{-i\hat{p}}$
$b^*_{\overline{p},\overline{q}}c_{\overline{p},\overline{q}}$	r_2
$b^*_{\overline{p},\overline{q}}a_{\overline{p},\overline{q}}$	$r_2e^{-i\hat{q}}$

$$Q^2_{\overline{p},\overline{q}}=\int dV_{\overline{p},\overline{q}}dV_{L_x-\overline{p},L_y^*-\overline{q}}\exp(H_{\overline{p},\overline{q}}+H^*_{L_x-\overline{p},L_y^*-\overline{q}}). \tag{50}$$

Here $H^*_{L_x-\overline{p},L_y^*-\overline{q}}$ can be obtained from $H_{\overline{p},\overline{q}}$ by replacing $\overline{p}$ by $L_x-\overline{p}$ and $\overline{q}$ by $L_y^*-\overline{q}$ for the Grassmann variables and replacing the coefficient in front of the Grassmann variables by its complex conjugate. The integration in Eq. (50) is very complicated, but the result turns out to be very simple and it yields

$$Q_{\overline{p},\overline{q}}=\left[A_0-A_1\cos\left(\frac{2\pi\overline{p}}{L_x}\right)-A_2\cos\left(\frac{2\pi\overline{q}}{L_y^*}\right)-A_3\cos\left(\frac{2\pi\overline{p}}{L_x}-\frac{2\pi\overline{q}}{L_y^*}\right)\right]^{1/2}, \tag{51}$$

with

$$A_0=1+r_1^2+r_2^2+r_3^2+r_1^2r_2^2+r_2^2r_3^2+r_1^2r_3^2+r_1^2r_2^2r_3^2+8r_1r_2r_3, \tag{52}$$

$$A_1=2r_1(1-r_2^2-r_3^2+r_2^2r_3^2), \tag{53}$$

$$A_2=2r_2(1-r_1^2-r_3^2+r_1^2r_3^2), \tag{54}$$

and

$$A_3=2r_3(1-r_1^2-r_2^2+r_1^2r_2^2). \tag{55}$$

Then the dimensionless free energy density on the infinitely long cylinder, defined as

$$f=-\lim_{L_y^*\to\infty}\frac{1}{N}\ln Q, \tag{56}$$

becomes

$$f=-C_1-\frac{C_2}{L_x}\sum_{\overline{p}}\int_0^{2\pi}\frac{d\phi}{2\pi}\ln\left[A_0-A_1\cos\left(\frac{2\pi\overline{p}}{L_x}\right)-A_2\cos\phi-A_3\cos\left(\frac{2\pi\overline{p}}{L_x}-\phi\right)\right], \tag{57}$$

with $C_1=\ln R_T$ and $C_2=\frac{1}{2}$ for a triangular lattice, and $C_1=\ln R_H$ and $C_2=\frac{1}{4}$ for a hexagonal lattice. Here the parameters A_0, A_1, A_2, and A_3, are given in terms of r_1, r_2, and r_3 by Eqs. (52)–(55) and vary with the lattices. We have $r_1=t_1$, $r_2=t_2$, and $r_3=0$ for a rectangular lattice; $r_1=t_1$, $r_2=t_2$, and $r_3=t_3$ for a triangular lattice. For a hexagonal lattice, we have

$$A_0=\alpha_0^2+\alpha_1^2+\alpha_2^2+\alpha_3^2, \tag{58}$$

$$A_1=2(\alpha_0\alpha_1-\alpha_2\alpha_3), \tag{59}$$

$$A_2=2(\alpha_0\alpha_2-\alpha_1\alpha_3), \tag{60}$$

and

$$A_3=2(\alpha_0\alpha_3-\alpha_1\alpha_2), \tag{61}$$

with α_0, α_1, α_2, and α_3 given by Eq. (11). Note that the relations given by the above equations for a hexagonal lattice can be verified to be the same as Eqs. (52)–(55) by substituting the relations of Eq. (11) into these equations. For the limit of $L_x\to\infty$, Eq. (57) becomes

$$f=-C_1-C_2\int_0^{2\pi}\frac{d\phi_1}{2\pi}\int_0^{2\pi}\frac{d\phi_2}{2\pi}\times\ln[A_0-A_1\cos\phi_1-A_2\cos\phi_2-A_3\cos(\phi_1-\phi_2)], \tag{62}$$

and the critical point is determined by the singular point of the free energy, $A_0-A_1-A_2-A_3=0$, which comes from the zero mode, $\overline{p}=0$ and $\overline{q}=0$, in Eq. (51).[10]

The expression of Eq. (57) for the free energy density can be further simplified by completing the integration. To obtain this, we reexpress Eq. (57) as

$$f=-C_1-\frac{C_2}{L_x}\sum_{\overline{p}}I(\overline{p}), \tag{63}$$

where the integration $I(\overline{p})$ is

$$I(\overline{p})=\int_0^{2\pi}\frac{d\phi}{2\pi}\ln[f_1(\overline{p})-X(\overline{p})\cos\phi-Y(\overline{p})\sin\phi], \tag{64}$$

with

$$f_1(\overline{p})=A_0-A_1\cos\frac{2\pi\overline{p}}{L_x}, \tag{65}$$

$$X(\overline{p})=A_2-A_3\cos\frac{2\pi\overline{p}}{L_x}, \tag{66}$$

and

$$Y(\overline{p})=A_3\sin\frac{2\pi\overline{p}}{L_x}. \tag{67}$$

By defining the angle Θ as

$$\tan\Theta = \frac{Y(\overline{p})}{X(\overline{p})}, \tag{68}$$

we can rewrite the integration as

$$I(\overline{p}) = \int_{-\Theta}^{2\pi-\Theta} \frac{d\Phi}{2\pi} \ln[f_1(\overline{p}) - f_2(\overline{p})\cos\Phi], \tag{69}$$

where the function $f_2(\overline{p})$ is

$$f_2(\overline{p}) = \sqrt{X^2(\overline{p}) + Y^2(\overline{p})}. \tag{70}$$

This integration can be completed, and the resultant free energy density is

$$f = -C_1 - \frac{C_2}{L_x} \sum_{\overline{p}} \ln \frac{f_1(\overline{p}) + \sqrt{f_1^2(\overline{p}) - f_2^2(\overline{p})}}{2}, \tag{71}$$

where the limits of the sum in $\overline{p}$ depend on the boundary condition and are specified previously after Eq. (45).

V. INTERFACIAL TENSION

The usual way of defining interfacial tension is as follows. Consider a $L_x \times L_y$ Ising rectangle with periodic boundary condition along L_y so that the geometry is a finite cylinder. Such an Ising system has either no domain walls or an even number of such walls for the cases where the boundary conditions along L_x are $++$ and $--$, respectively. Here the boundary condition $++$ $(--)$ refers to the situation in which the Ising spins on the left and on the right have fixed value $\sigma = +1$ (-1). On the other hand, for the $+-$ boundary condition in which the Ising spins are specified as $+1$ on the left and -1 on the right, the system has an odd number of domain walls. Then comparing with the boundary conditions $++$ or $--$ the system with the $+-$ boundary condition has excess free energy caused by domain walls, and for low enough temperatures it is conjectured that the excess free energy is caused exactly by one domain wall in the thermodynamic limit.[13] Thus the interfacial tension, which is the excess free energy per site and per $k_B T$, is

$$\tau(\theta, R, L_x) = L_x[f_{+-}(\theta, R, L_x) - f_{++}(\theta, R, L_x)], \tag{72}$$

where θ is the reduced temperature $\theta = (T - T_c)/T_c$, R is the aspect ratio $R = L_y/L_x$, f_{+-} is the free energy density per $k_B T$ with the $+-$ boundary condition, and f_{++} is that with the $++$ boundary condition. In the limit L_x, $L_y \to \infty$ with fixed R, the quantity $\tau(\theta, R, L_x)$ approaches the bulk interfacial tension $\tau^b(\theta)$ which vanishes for $\theta \geqslant 0$, and $\tau^b(\theta) \sim (-\theta)^\mu$ for $\theta < 0$. Here μ is the critical index for the interfacial tension, and its value is 1 for the two-dimensional Ising model.

In this work we extend the above consideration to a different situation. Similar to the above case, we consider two $L_x \times L_y$ Ising rectangles that both have a periodic boundary condition along L_y. But the boundary conditions along L_x are periodic and antiperiodic, respectively, and hence the geometric shapes are toruses. Note that for the antiperiodic boundary along L_x the spins between the first and the last rows at the same column have antiferromagnetic couplings.

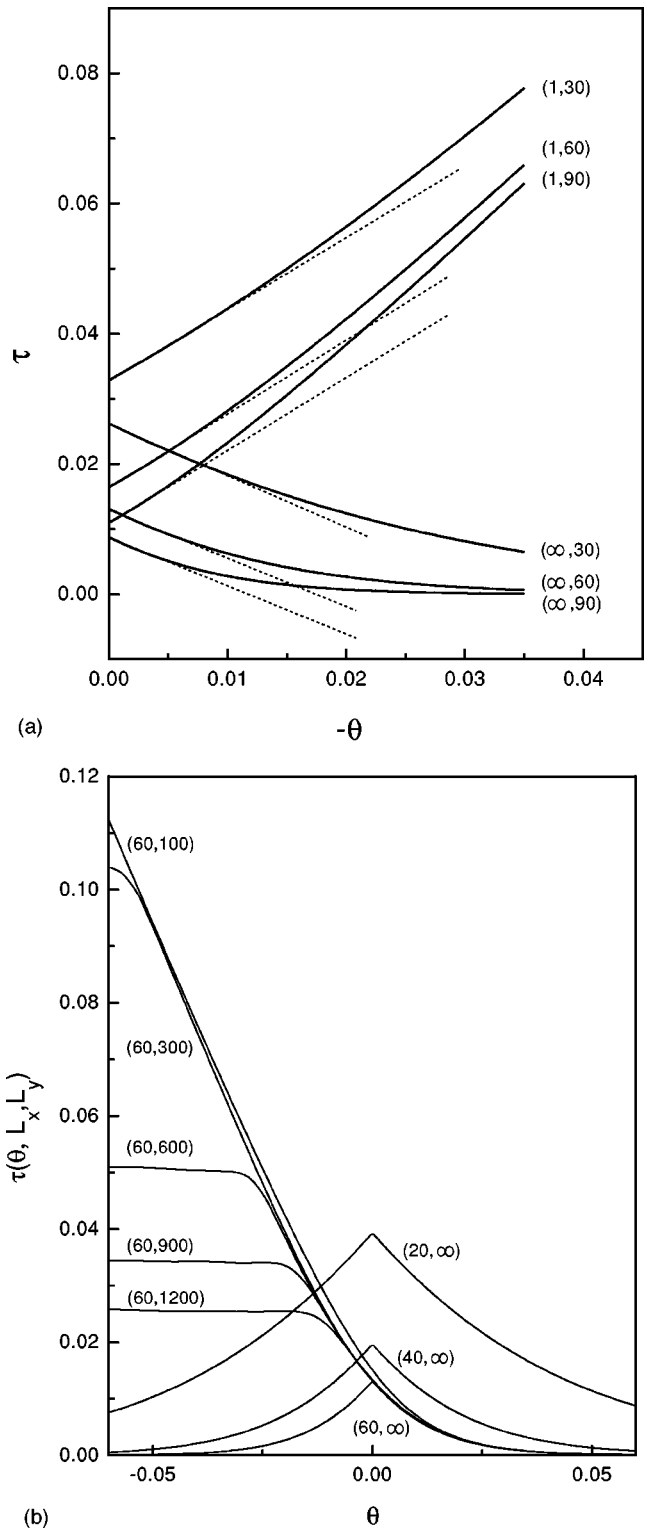

FIG. 3. The interfacial tension τ for square lattices with isotropic coupling as a function of the reduced temperature $\theta = (T - T_c)/T_c$ calculated from Eq. (74) (solid lines) for (a) given values of (R, L_x) with aspect ratio R, and (b) given values of (L_x, L_y). The dotted lines in (a) are from the relation $\tau = a - b\theta$ with constant a and b.

Both systems have either no domain walls or an even number of such walls, and hence the physical situation here is different from the usual case defined previously. But comparing with the case of periodic boundary conditions on both sides, the system with a periodic boundary condition

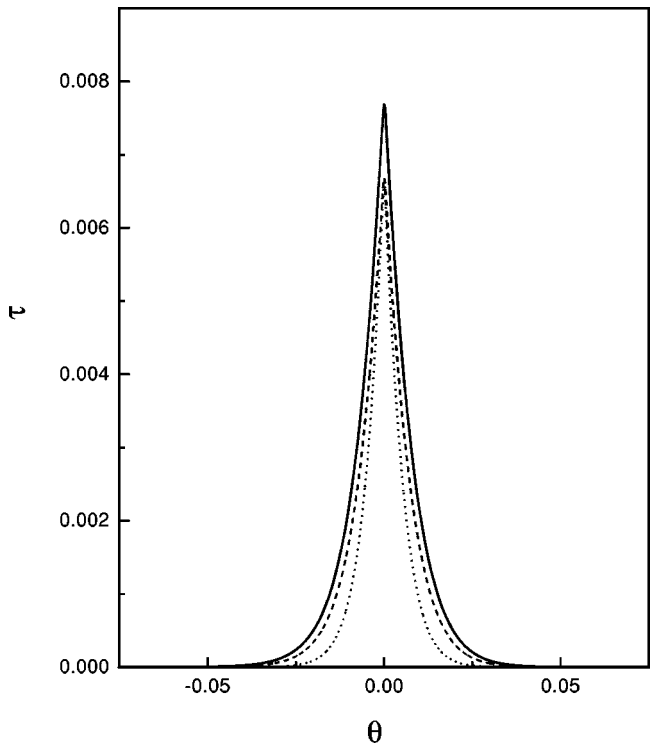

FIG. 4. The interfacial tensions τ as a function of the reduced temperature θ for infinitely long cylinders of a rectangular (solid line), triangular (dashed line), and hexagonal (dotted line) lattices. The couplings are isotropic, and the circumference of the cylinder is $L_x=100$.

on one side and an antiperiodic boundary condition on the other side may still have excess free energy caused by the additional antiferromagnetic layer. Thus, similar to Eq. (72), for the isotropic couplings we define the interfacial tension as

$$\tau(\theta,R,L_x)=L_x[f_{ap}(\theta,R,L_x)-f_{pp}(\theta,R,L_x)], \qquad (73)$$

where f_{ap} is the free energy density per k_BT with an antiperiodic boundary condition along L_x and a periodic boundary condition along L_y, and f_{pp} is that with a periodic boundary condition on both sides. The analytical expression of the interfacial tension was obtained to have the form[14]

$$\tau(\theta,R,L_x)=\frac{1}{L_y}\ln\left[\frac{\alpha_1+\alpha_2+\alpha_3-\mathrm{sgn}(\theta)\alpha_4}{\alpha_1-\alpha_2+\alpha_3+\mathrm{sgn}(\theta)\alpha_4}\right], \qquad (74)$$

where

$$\alpha_1=\prod_{p=0}^{L_x-1}\prod_{q=0}^{L_y-1}\left[\lambda_0-\lambda_1\left(\cos\frac{2\pi p+\pi}{L_x}+\cos\frac{2\pi q+\pi}{L_y}\right)\right]^{1/2}, \qquad (75)$$

$$\alpha_2=\prod_{p=0}^{L_x-1}\prod_{q=0}^{L_y-1}\left[\lambda_0-\lambda_1\left(\cos\frac{2\pi p+\pi}{L_x}+\cos\frac{2\pi q}{L_y}\right)\right]^{1/2}, \qquad (76)$$

TABLE II. The values of the parameters in the scaling function, $\Sigma(z;r_{21})=a_{N_x}(r_{21})+b(r_{21})z$, with $a_{N_x}(r_{21})=A(r_{21})[1+a_1(r_{21})x^2+\cdots]$ and $x=1/N_x$, for an Ising cylinder of the rectangular lattice with different coupling ratio r_{21}.

r_{21}	θ_c	$A(r_{21})$	$a_1(r_{21})$	$b(r_{21})$
8	7.778 755 996(9)	3.0213(1)	3.259(5)	−1.510(4)
7	7.112 386 204(1)	2.7565(5)	2.747(9)	−1.470(1)
6	6.423 824 381(0)	2.4823(2)	2.281(5)	−1.429(8)
5	5.707 791 440(4)	2.1962(2)	1.831(3)	−1.361(6)
4	4.956 310 931(2)	1.8944(9)	1.416(8)	−1.278(9)
3	4.156 173 778(9)	1.5707(9)	1.043(3)	−1.202(1)
2	3.282 035 818(1)	1.2124(0)	0.692(0)	−1.081(3)
1	2.269 185 283(4)	0.7853(9)	0.411(3)	−0.879(0)
$\frac{1}{2}$	1.641 017 906(5)	0.5087(8)	0.292(4)	−0.696(6)
$\frac{1}{3}$	1.385 391 270(5)	0.3927(0)	0.257(5)	−0.599(2)
$\frac{1}{4}$	1.239 077 730(2)	0.3256(0)	0.241(5)	−0.533(8)
$\frac{1}{5}$	1.141 558 295(8)	0.2808(7)	0.232(5)	−0.485(3)
$\frac{1}{6}$	1.070 637 394(9)	0.2484(9)	0.227(3)	−0.447(7)
$\frac{1}{7}$	1.016 055 166(4)	0.2237(7)	0.223(3)	−0.418(0)
$\frac{1}{8}$	0.972 344 505(3)	0.2041(7)	0.220(0)	−0.393(3)

$$\alpha_3=\prod_{p=0}^{L_x-1}\prod_{q=0}^{L_y-1}\left[\lambda_0-\lambda_1\left(\cos\frac{2\pi p}{L_x}+\cos\frac{2\pi q+\pi}{L_y}\right)\right]^{1/2}, \qquad (77)$$

$$\alpha_4=\prod_{p=0}^{L_x-1}\prod_{q=0}^{L_y-1}\left[\lambda_0-\lambda_1\left(\cos\frac{2\pi p}{L_x}+\cos\frac{2\pi q}{L_y}\right)\right]^{1/2}, \qquad (78)$$

$\lambda_0=(1+t^2)^2$, and $\lambda_1=2t(1-t^2)$, with $J_1=J_2=J$ and $t=\tanh(\beta J)$. Note that the sign factor in front of the last term of Eq. (74) is equal to $+1$ for $\theta>0$ and -1 for $\theta<0$. Some results calculated from Eq. (74) are shown in Fig. 3. We find that the interfacial tension agrees very well with the relation $\tau=a+b(-\theta)^{\mu}$ for $\theta<0$ and $\mu=1$, as shown in Fig. 3(a). However, when we fix the L_x size to be 60 and increase the L_y size, the behavior of τ changes dramatically and approaches that in an infinitely long cylinder for $L_y\geqslant 1500$ as shown in Fig. 3(b). This dramatic change in the behavior of τ may be caused by the suppression of the fluctuation of the antiferromagnetic layer for sufficiently large L_y. For an infinitely long cylinder as shown also in Fig. 3(b), the peak of τ is located exactly at the critical point, the value of τ decreases in a symmetrical way from the critical point, and the distribution of τ becomes more sharp but with the same critical index $\mu=1$ when the L_x size is decreased.[14] These features may be understood in the following way. In a low enough temperature, the spin configuration with all the spins up or down, which gives the lowest energy to the case of a periodic boundary condition, also gives the lowest energy to the case of an antiperiodic boundary, and hence the interfacial tension tends to vanish. However, the free energy density at the critical point for the case of an antiperiodic boundary condition given by Eq. (57) contains the zero mode (i.e., $\phi=0$ and $\bar{p}=L_x$), and this is responsible for the rise of the peak. Similar to the finite case, for the infinite cylinder we have the peak decreased when the L_x size increases, and this

TABLE III. The values of the parameters in the scaling function, $\Sigma(z;r_{21},r_{31})=a_{N_x}(r_{21},r_{31})+b(r_{21},r_{31})z$, with $a_{N_x}(r_{21},r_{31})=A(r_{21},r_{31})[1+a_1(r_{21},r_{31})x^2+\cdots]$ and $x=1/N_x$, for an Ising cylinder of the triangular lattice with different coupling ratios r_{21} and r_{31}.

r_{21}	r_{31}	θ_c	$A(r_{21},r_{31})$	$a_1(r_{21},r_{31})$	$b(r_{21},r_{31})$
3	5	10.464 490 200(2)	0.4584(5)	−0.099(5)	−0.670(8)
3	4	9.421 100 552(0)	0.4801(4)	−0.109(1)	−0.687(6)
3	3	8.312 347 584(8)	0.4995(2)	−0.111(7)	−0.704(0)
3	2	7.12 386 086(0)	0.5100(7)	−0.072(9)	−0.710(2)
3	1	5.770 780 116(4)	0.4936(5)	0.027(1)	−0.693(9)
3	$\frac{1}{2}$	5.013 521 949(8)	0.4608(1)	0.132(4)	−0.664(2)
3	$\frac{1}{3}$	4.741 590 822(9)	0.44431(6)	0.174(4)	−0.648(5)
3	$\frac{1}{4}$	4.600 956 724(0)	0.4326(5)	0.193(0)	−0.638(0)
3	$\frac{1}{5}$	4.514 901 660(4)	0.4257(3)	0.209(3)	−0.632(1)
2	5	9.105 411 127(5)	0.4396(8)	−0.030(5)	−0.652(2)
2	4	8.138 513 891(1)	0.4729(5)	−0.056(0)	−0.680(8)
2	3	7.112 386 086(0)	0.5100(7)	−0.072(9)	−0.710(2)
2	2	6.003 554 752(3)	0.5479(5)	−0.080(3)	−0.739(0)
2	1	4.766 243 976(4)	0.5719(0)	−0.004(2)	−0.752(7)
2	$\frac{1}{2}$	4.069 256 947(4)	0.5620(7)	0.108(5)	−0.742(1)
2	$\frac{1}{3}$	3.819 300 277(9)	0.5511(6)	0.163(1)	−0.732(3)
2	$\frac{1}{4}$	3.690 116 851(2)	0.5435(3)	0.191(5)	−0.727(2)
2	$\frac{1}{5}$	3.611 101 260(6)	0.5381(2)	0.213(1)	−0.722(3)
1	5	7.575 056 002(7)	0.3916(2)	0.083(2)	−0.603(4)
1	4	6.699 628 590(4)	0.4359(0)	0.058(7)	−0.644(3)
1	3	5.770 780 116(4)	0.4936(5)	0.027(1)	−0.694(9)
1	2	4.766 243 976(4)	0.5719(0)	0.004(2)	−0.752(8)
1	1	3.640 956 876(2)	0.6801(7)	0.001(0)	−0.823(1)
1	$\frac{1}{2}$	3.001 777 392(7)	0.7437(4)	0.091(3)	−0.860(1)
1	$\frac{1}{3}$	2.770 782 536(3)	0.7632(0)	0.158(8)	−0.869(6)
1	$\frac{1}{4}$	2.650 888 491(0)	0.7716(3)	0.202(3)	−0.874(4)
1	$\frac{1}{5}$	2.577 356 032(8)	0.7760(3)	0.235(9)	−0.876(6)
$\frac{1}{2}$	5	6.703 889 888(0)	0.3476(0)	0.163(1)	−0.562(3)
$\frac{1}{2}$	4	5.884 122 697(0)	0.3947(3)	0.146(2)	−0.604(9)
$\frac{1}{2}$	3	5.013 521 949(8)	0.4608(1)	0.132(4)	−0.664(2)
$\frac{1}{2}$	2	4.069 256 947(4)	0.5620(7)	0.108(5)	−0.742(1)
$\frac{1}{2}$	1	3.001 777 392(7)	0.7437(4)	0.091(3)	−0.860(1)
$\frac{1}{2}$	$\frac{1}{2}$	2.383 121 980(6)	0.9089(4)	0.144(5)	−0.948(2)
$\frac{1}{2}$	$\frac{1}{3}$	2.154 752 616(2)	0.9875(7)	0.214(1)	−0.985(4)
$\frac{1}{2}$	$\frac{1}{4}$	2.034 628 476(9)	1.0337(7)	0.276(3)	−1.005(8)
$\frac{1}{2}$	$\frac{1}{5}$	1.960 277 937(3)	1.0642(0)	0.322(1)	−1.019(1)
$\frac{1}{3}$	5	6.389 269 794(0)	0.3283(9)	0.190(0)	−0.539(5)
$\frac{1}{3}$	4	5.590 457 061(5)	0.3755(3)	0.180(8)	−0.587(2)
$\frac{1}{3}$	3	4.741 590 822(9)	0.4431(6)	0.176(7)	−0.648(5)
$\frac{1}{3}$	2	3.819 300 277(9)	0.5511(6)	0.175(7)	−0.732(6)
$\frac{1}{3}$	1	2.770 782 536(3)	0.7632(0)	0.158(8)	−0.869(6)
$\frac{1}{3}$	$\frac{1}{2}$	2.154 752 616(2)	0.9875(7)	0.214(1)	−0.985(5)
$\frac{1}{3}$	$\frac{1}{3}$	1.923 593 864(8)	1.1107(2)	0.291(7)	−1.038(7)
$\frac{1}{3}$	$\frac{1}{4}$	1.800 587 707(0)	1.1899(3)	0.361(6)	−1.071(0)
$\frac{1}{3}$	$\frac{1}{5}$	1.723 802 091(0)	1.2455(0)	0.423(3)	−1.092(3)

TABLE IV. The values of the parameters in the scaling function, $\Sigma(z;r_{21},r_{31})=a_{N_x}(r_{21},r_{31})+b(r_{21},r_{31})z$, with $a_{N_x}(r_{21},r_{31})=A(r_{21},r_{31})[1+a_1(r_{21},r_{31})x^2+\cdots]$ and $x=1/N_x$, for an Ising cylinder of the hexagonal lattice with different coupling ratios r_{21} and r_{31}.

r_{21}	r_{31}	θ_c	$A(r_{21},r_{31})$	$a_1(r_{21},r_{31})$	$b(r_{21},r_{31})$
3	5	3.679 615 323(3)	0.8333(6)	0.701(5)	−0.779(1)
3	4	3.462 985 702(8)	0.8540(0)	0.532(1)	−0.820(1)
3	3	3.159 685 820(5)	0.8797(9)	0.234(9)	−0.855(7)
3	2	2.729 042 824(5)	0.9040(7)	−0.189(3)	−0.868(8)
3	1	2.078 086 900(5)	0.8781(0)	−0.630(3)	−0.806(6)
3	$\frac{1}{2}$	1.579 842 912(5)	0.7509(5)	−0.466(1)	−0.677(9)
3	$\frac{1}{3}$	1.355 032 037(9)	0.6450(6)	−0.173(4)	−0.591(9)
3	$\frac{1}{4}$	1.220 860 463(5)	0.5652(9)	0.056(1)	−0.530(9)
3	$\frac{1}{5}$	1.129 383 577(4)	0.5041(4)	0.018(9)	−0.485(1)
2	5	3.074 559 426(4)	1.0392(5)	0.944(3)	−0.837(5)
2	4	2.939 116 469(2)	1.0513(6)	0.772(8)	−0.889(4)
2	3	2.729 042 824(5)	1.0654(4)	0.496(4)	−0.943(5)
2	2	2.405 456 680(5)	1.0701(0)	0.037(1)	−0.980(4)
2	1	1.884 525 563(7)	0.9990(4)	−0.443(7)	−0.931(9)
2	$\frac{1}{2}$	1.469 558 234(8)	0.8220(1)	−0.324(6)	−0.785(8)
2	$\frac{1}{3}$	1.277 843 623(4)	0.6920(6)	−0.058(6)	−0.680(8)
2	$\frac{1}{4}$	1.161 682 666(5)	0.5989(6)	0.011(8)	−0.605(5)
2	$\frac{1}{5}$	1.081 552 639(2)	0.5296(1)	0.237(6)	−0.548(3)
1	5	2.228 707 560(8)	1.5703(9)	1.547(0)	−0.947(7)
1	4	2.179 079 795(0)	1.5687(6)	1.400(5)	−1.000(5)
1	3	2.078 086 900(4)	1.5610(7)	1.127(6)	−1.075(2)
1	2	1.884 525 563(7)	1.5263(9)	0.635(6)	−1.152(1)
1	1	1.518 651 422(3)	1.3603(4)	0.011(2)	−1.139(5)
1	$\frac{1}{2}$	1.202 728 340(5)	1.0701(0)	0.046(1)	−0.979(8)
1	$\frac{1}{3}$	1.053 228 607(8)	0.8798(0)	0.224(6)	−0.854(6)
1	$\frac{1}{4}$	0.962 116 467(2)	0.7499(9)	0.366(9)	−0.762(7)
1	$\frac{1}{5}$	0.899 143 260(4)	0.6560(7)	0.482(9)	−0.692(4)
$\frac{1}{2}$	5	1.634 866 759(0)	2.4215(1)	2.744(9)	−1.101(7)
$\frac{1}{2}$	4	1.621 073 685(0)	2.4138(6)	2.657(4)	−1.136(7)
$\frac{1}{2}$	3	1.579 842 912(5)	2.3889(9)	2.406(8)	−1.209(4)
$\frac{1}{2}$	2	1.469 558 234(8)	2.3066(2)	1.799(6)	−1.316(5)
$\frac{1}{2}$	1	1.202 728 340(5)	1.9968(4)	0.831(8)	−1.338(6)
$\frac{1}{2}$	$\frac{1}{2}$	0.942 262 781(9)	1.5264(0)	0.628(6)	−1.151(4)
$\frac{1}{2}$	$\frac{1}{3}$	0.813 906 957(1)	1.2398(4)	0.722(7)	−0.998(7)
$\frac{1}{2}$	$\frac{1}{4}$	0.734 779 119(9)	1.0513(6)	0.771(3)	−0.888(0)
$\frac{1}{2}$	$\frac{1}{5}$	0.679 874 711(1)	0.9179(0)	0.807(0)	−0.804(6)
$\frac{1}{3}$	5	1.383 523 162(2)	3.1393(1)	4.059(5)	−1.212(6)
$\frac{1}{3}$	4	1.377 673 355(1)	3.1320(8)	4.010(2)	−1.236(1)
$\frac{1}{3}$	3	1.355 032 037(9)	3.1032(0)	3.789(3)	−1.298(5)
$\frac{1}{3}$	2	1.277 843 623(4)	2.9930(8)	3.102(8)	−1.415(9)
$\frac{1}{3}$	1	1.053 228 607(8)	2.5639(1)	1.726(7)	−1.459(2)
$\frac{1}{3}$	$\frac{1}{2}$	0.813 906 957(1)	1.9325(0)	1.212(4)	−1.247(0)
$\frac{1}{3}$	$\frac{1}{3}$	0.692 695 635(7)	1.5160(6)	1.133(8)	−1.074(1)
$\frac{1}{3}$	$\frac{1}{4}$	0.617 535 937(8)	1.3218(4)	1.100(2)	−0.951(9)
$\frac{1}{3}$	$\frac{1}{5}$	0.565 397 928(1)	1.1546(9)	1.071(0)	−0.862(1)

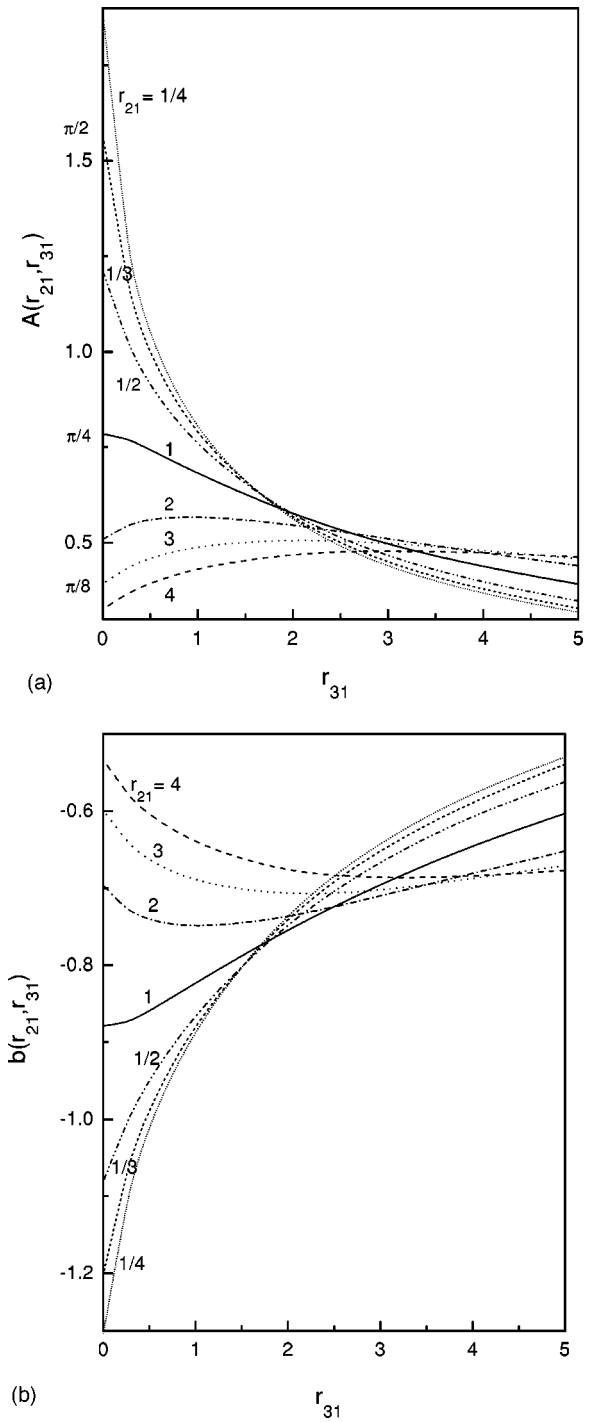

FIG. 5. The scaling function of the interfacial tension is defined as $\Sigma(\theta N_x^{1/\nu};r_{21},r_{31})=A(r_{21},r_{31})\cdot[1+a_1(r_{21},r_{31})/N_x^2+\cdots]+b(r_{21},r_{31})\cdot(\theta N_x^{1/\nu})$. (a) The $A(r_{21},r_{31})$ vs r_{31} curve for a given value of r_{21}, and (b) the $b(r_{21},r_{31})$ vs r_{31} curve for a given value of r_{21}, for triangular lattices. The data points at $r_{31}=0$ correspond to the case of the rectangular lattice.

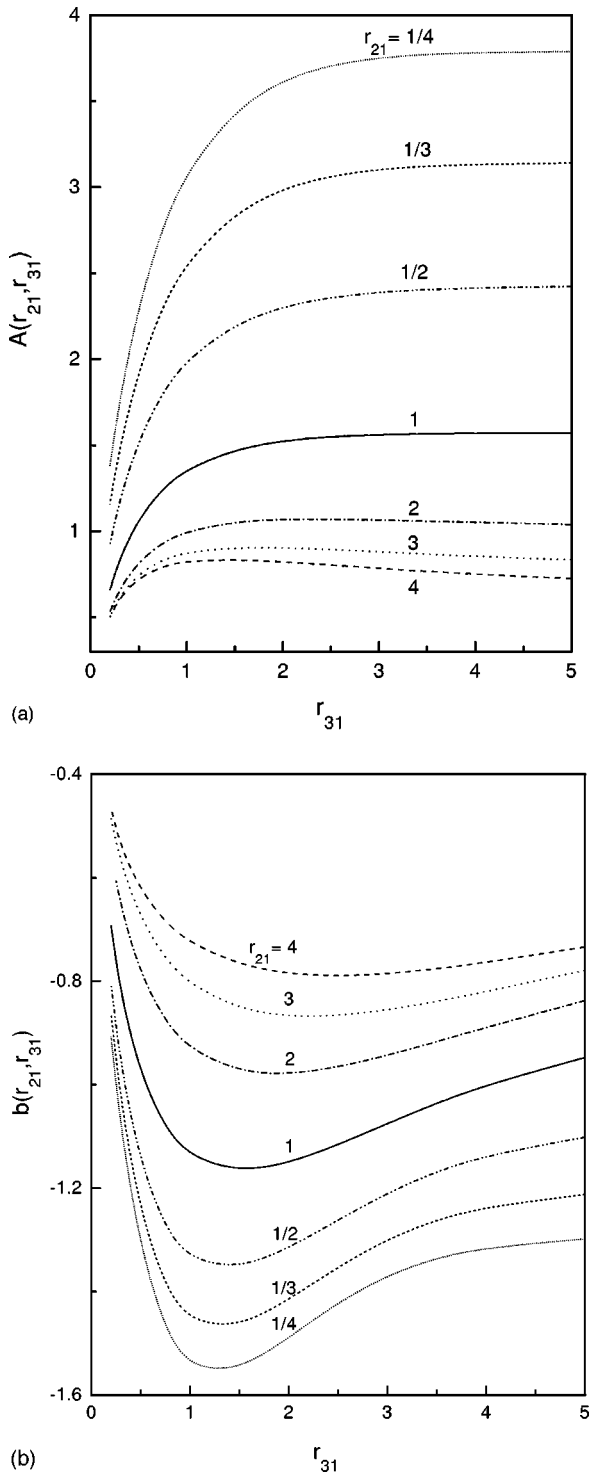

FIG. 6. The scaling function of the interfacial tension is defined as $\Sigma(\theta N_c^{1/\nu};r_{21},r_{31})=A(r_{21},r_{31})\cdot[1+a_1(r_{21},r_{31})/N_x^2+\cdots]+b(r_{21},r_{31})\cdot(\theta N_x^{1/\nu})$. (a) The $A(r_{21},r_{31})$ vs r_{31} curve for a given value of r_{21}, and (b) the $b(r_{21},r_{31})$ vs r_{31} curve for a given value of r_{21}, for hexagonal lattices.

is again due to the suppression of the fluctuation of the antiferromagnetic layer. In the following, we analyze the coupling-anisotropy and finite-size effects in the scaling functions of the interfacial tensions based on the analytical expressions of free energies obtained in the last section. Because the value of τ decreases in a symmetrical way from the critical point, we restrict our analysis to the ordered phase.

For a class of Ising cylinders discussed in the previous sections, we define the interfacial tension as

$$\tau(\theta,r_{21},r_{31};N_x)=N_x[f_a(\theta,r_{21},r_{31};N_x)-f_p(\theta,r_{21},r_{31};N_x)], \quad (79)$$

where f_a is the free energy density per k_BT for the circumference joined antiperiodically, f_p is for the circumference joined periodically, N_x is the number of sites along the circumference, and the coupling ratios r_{21} and r_{31} are defined as $r_{21}=J_2/J_1$ and $r_{31}=J_3/J_1$. Note that we choose the coupling constant J_1 as the scale to measure the temperature and to define the coupling ratios, and N_x is L_x for a triangular lattice, $2L_x$ for a hexagonal lattice. Then from Eq. (73) we have

$$\tau(\theta,r_{21},r_{31};N_x) = \frac{1}{2}\sum_{p=1}^{L_x} \ln\left[\frac{f_1(p+\frac{1}{2})+\sqrt{f_1^2(p+\frac{1}{2})-f_2^2(p+\frac{1}{2})}}{f_1(p)+\sqrt{f_1^2(p)-f_2^2(p)}}\right]. \tag{80}$$

The numerical results of this equation for three types of lattices with isotropic couplings and $L_x=100$ are shown in Fig. 4.

From the usual scaling ansatz, we can write the scaling form of τ as

$$\tau(\theta,r_{21},r_{31};N_x)=N_x^{-1}\Sigma(\theta N_x^{1/\nu};r_{21},r_{31}), \tag{81}$$

where $\Sigma(z;r_{21},r_{31})$ with $z=\theta N_x^{1/\nu}$ is the scaling function. We then employ the form

$$\Sigma(z;r_{21},r_{31})=a_{N_x}(r_{21},r_{31})+b(r_{21},r_{31})z, \tag{82}$$

to approximate the scaling function. There is a finite-size correction in a_{N_x} due to the finite size N_x, and we define $A(r_{21},r_{31})$ as the value of $a_{N_x}(r_{21},r_{31})$ in the limit of large N_x,

$$A(r_{21},r_{31})\equiv\lim_{N_x\gg} a_{N_x}(r_{21},r_{31}). \tag{83}$$

The value of A is referred to the amplitude of σ at the critical point. The finite-size dependence of the value of a_{N_x} is determined by fitting to the form of

$$a_{N_x}(r_{21},r_{31})=A(r_{21},r_{31})[1+a_1(r_{21},r_{31})x^2+\cdots], \tag{84}$$

with $x=1/N_x$. The leading order of the finite-size effect is the order of $1N_x^2$, and this reflects the fact that the finite-size correction is very small.

For isotropic couplings, the values of A, a_1, and b are $\pi/4$, 0.411(3), and $-0.879(0)$ for a rectangular lattice, 0.6801(7), 0.001(0), and $-0.823(1)$ for a triangular lattice, and 1.3603(4), 0.011(2), and $-1.139(5)$ for a hexagonal lattice. For anisotropic couplings, the values of A, a_1, and b are listed in Table II for a rectangular lattice, in Table III for a triangular lattice, and in Table IV for a hexagonal lattice. The qualitative behaviors of A and b as functions of r_{31} for a specified value of r_{21} are shown in Fig. 5 for a triangular lattice and in Fig. 6 for a hexagonal lattice. Note that in Fig. 5(a) the values for a triangular lattice at $r_{31}=0$ and the given r_{21} correspond to the values for a rectangular lattice at the given r_{21}.

VI. SUMMARY

We work in the framework of Plechko's Grassmann path-integral factorization of the Boltzmann weights with the principle of mirror ordering of the arising Grassmann factors to obtain the analytic solutions for Ising cylinders of rectangular, triangular, and hexagonal lattices. To deal with the boundary conditions imposed on the joined circumferences of the cylinders, which are periodic or antiperiodic, we introduce three pairs of conjugate Grassmann variables on a lattice site. Then we use the analytic solutions to study the scaling functions of the interfacial tensions, and the results are summarized in the following way:

(i) The peaks of the interfacial tensions are located exactly at the critical point, and then their values decrease in a symmetrical way from the critical point.

(ii) The scaling functions of the interfacial tensions are expressed as $\Sigma(z;r_{21},r_{31})=a_{N_x}(r_{21}+r_{31})+b(r_{21},r_{31})z$ with $z=\theta N_x^{1/\nu}$, $r_{21}=J_2/J_1$, and $r_{31}=J_3/J_1$. We determine the values of the parameters a_{N_x} and b, for various coupling ratios on three types of lattices. Our results indicate that the finite-size correction to the values of a_{N_x} is very small, and it is extremely small on triangular lattice.

(iii) If the finite-size correction is neglected, the interfacial tensions can be rearranged to the form of

$$\tau(\theta,r_{21},r_{31};N_x)=b(r_{21},r_{31})\,\theta^{1/\nu}\left[1+\frac{1}{N_x\theta^{1/\nu}}\frac{A(r_{21},r_{31})}{b(r_{21},r_{31})}\right]. \tag{85}$$

This form gives the scaling function

$$F(x)=1+\frac{B}{x}, \tag{86}$$

with $x=N_x\theta^{1/\nu}$, used by Mon and Jasnow.[3] For the isotropic couplings, the value of B is $-0.893(5)$ for a rectangular lattice, $-0.826(4)$ for a triangular lattice, and $-1.193(8)$ for a hexagonal lattice.

ACKNOWLEDGMENTS

The authors wish to thank V. N. Plechko for valuable discussions and a critical reading of the paper. This work was partially supported by the National Science Council of Republic of China (Taiwan) under Grant No. NSC 88-2112-M-033-002.

[1] H. Park and M. den Nijs, Phys. Rev. B **38**, 565 (1988).
[2] V. Privman and M. E. Fisher, J. Stat. Phys. **33**, 385 (1983).
[3] K. K. Mon and D. Jasnow, Phys. Rev. A **30**, 670 (1984); **31**, 4008 (1985).
[4] L. Onsager, Phys. Rev. **65**, 117 (1944).
[5] B. Kaufman, Phys. Rev. **76**, 1232 (1949).
[6] T. D. Shultz, D. C. Mattis, and E. H. Lieb, Rev. Mod. Phys. **36**, 856 (1964).
[7] M. Kac and J. C. Ward, Phys. Rev. **88**, 1332 (1952).
[8] H. S. Green and C. A. Hurst, *Order-Disorder Phenomena* (Inter-

science, New York, 1964).
[9] V. N. Plechko, Theor. Math. Phys. **64**, 748 (1985).
[10] V. N. Plechko, Physica A **152**, 51 (1988).
[11] V. N. Plechko, Phys. Lett. A **157**, 335 (1991).
[12] F. A. Berezin, *The Method of Second Quantization* (Academica, New York, 1966).
[13] D. B. Abraham and N. M. Svrakic, Phys. Rev. Lett. **56**, 1172 (1986).
[14] M. C. Wu, M. C. Huang, Y. P. Luo, and T. M. Liaw, J. Phys. A **32**, 4897 (1999).